Article

Hybrid siliconized–epoxidized EPDM/polyurethane (eEPDM-*g*-APTES/HTPDMS/PU) matrices for potential application in cable insulation

Manokaran Vadivel[1] , Moses Suresh Chandra Kumar[2],
Jabbar Abbas Mohaideen[1], Muthukaruppan Alagar[3],
Murugesan Sankarganesh[4] and Jeyaraj Dhaveethu Raja[5]

Abstract
Hybrid matrices (epoxidized of ethylene–propylene–diene monomer (eEPDM)-*g*-aminopropyltriethoxysilane (APTES)/hydroxyl terminated polydimethylsiloxane (HTPDMS)/polyurethane (PU)) were developed based on eEPDM with 3-APTES coupling agent and varying weight percentages (0.75, 1.50, 2.25, and 3.00 wt%) of PU prepolymer as coreactant using 7.5 wt% of HTPDMS as chain extender using suitable experimental conditions. The formation of hybrid matrices and their structure were characterized by Fourier transform infrared (FTIR). The thermal and morphological properties of the hybrid matrices were analyzed using differential scanning calorimetry and scanning electron microscope, respectively. Mechanical properties (tensile strength, elongation at break (%), Young's modulus, and hardness) were characterized as per ASTM standards. Data resulted from mechanical studies, it was noticed that the incorporation of 3-APTES, HTPDMS, and PU into eEPDM has improved the elongation at break (%) and lowered the values of tensile strength, Young's modulus, and hardness according to the percentage concentration. Morphological studies indicate the presence of heterogeneous morphology. Data obtained from different studies, it suggested that the hybrid matrices developed in the present work can be used as cable insulates for high-performance industrial and engineering applications.

Introduction

Polymer composites slow down the defects of polymer main structures and also possess an outstanding tensile and inter-laminar strength related properties.[1–7] Ethylene–propylene–diene monomer (EPDM) is one of the most versatile synthetic elastomers used for the number of industrial, engineering, and commercial applications[8–11] because of its outstanding resistance to oxidation,[12] ozone,[13,14] and the effects of weathering and wide range of operating temperature over other available synthetic commercial elastomers.[15] The attractive combination of performance characteristics makes EPDM unique among synthetic elastomers and has ensured its use in an impressive and wide range of technical components, including

[1] Chemistry Research Centre, Mohamed Sathak Engineering College, Kilakarai, Ramanathapuram (Dist), Tamil Nadu, India
[2] Polymer Nanocomposite Centre, Scott Christian College, Nagercoil, Kanyakumari (Dist), Tamil Nadu, India
[3] Polymer Engineering Laboratory, PSG Institute of Technology and Applied Research, Neelambur, Coimbatore, Tamil Nadu, India
[4] Department of Chemistry, K. Ramakrishnan College of Technology, Samayapuram, Trichy, Tamil Nadu, India
[5] Department of Chemistry, The American College, Tallakkulam, Madurai, Tamil Nadu, India

Corresponding authors:
Manokaran Vadivel, Chemistry Research Centre, Mohamed Sathak Engineering College, Kilakarai, Ramanathapuram (Dist), Tamil Nadu 623 806, India.
Email: vadivelche@gmail.com

Muthukaruppan Alagar, Polymer Engineering Laboratory, PSG Institute of Technology and Applied Research, Neelambur, Coimbatore 641 062, Tamil Nadu, India.
Email: mkalagar@yahoo.com

freezer gaskets,[16] O-rings,[17] air-craft seals,[18] rocket engine insulation,[19] ablative insulation materials,[20,21] cable insulation materials,[22,23] and cable for power transmission.[24] Though EPDM possesses good characteristic properties, still it is considered as general-purpose elastomer.[25] Hence, to make EPDM as cost competitive high-performance speciality elastomer suitable for wide range of industrial applications,[26] an attempt has been made in the present work to improve certain selected characteristics of EPDM, namely, range of service temperature, elongation at break (%), char yield (%), flame retardant behavior, and dielectric character, and to improve the flexibility by reducing its hardness by incorporating both hydroxyl terminated polydimethylsiloxane (HTPDMS) and polyurethane (PU) prepolymer through silane coupling agent. In the present work, hybrid materials were developed based on epoxidized ethylene–propylene–diene monomer (eEPDM) with varying weight percentages (1.50, 2.0, 2.5, and 3 wt%) of 3-aminopropyltriethoxysilane (APTES) as coupling agent and varying weight percentages (0.75, 1.50, 2.25, and 3 wt%) of PU prepolymer as coreactant using 0.75 wt% of HTPDMS as chain extender under appropriate experimental conditions and their properties were characterized by different analytical methods. Data resulted from different studies are discussed and reported.

Experimental

Materials

The EPDM (ethylidene norbornene type diene) terpolymer used in this study was a commercial grade Nordel IP 4750 R supplied by Du Pont's Dow elastomers, Stow, Ohio, USA (ethylene/propylene/5-ethylidene-2-norbornene: 71/20/9 by wt% and specific gravity of 0.88). 3-APTES (Sigma-Aldrich, St Louis, Missouri, USA; boiling point = 217°C, density = 0.946 g cm^{-3}, and M_w = 221.3) is used as a silane grafting agent. Polypropyleneglycol (PPG 400) was procured from Merck Specialties Pvt Ltd, Mumbai, Maharashtra, India (M_w = 200 and density = 1.1264). Toluene diisocyanate (TDI; M_w = 174.16, 80/20 mixture of 2,4 and 2,6 TDI isomers, NCO index = 47.5 eq kg^{-1}) was procured from MPL, Chennai, India. Dibutyltindilaurate (DBTDL, Merck, Germany, density = 1.066 g cm^{-3}, freezing point >110°C, M_w = 631.56) and octamethylcyclotetrasiloxane (boiling point = 176°C, density = 0.956 g cm^{-3}, refractive index = 1.396, viscosity = 25 cP at 25°C, M_w = 296.6) were purchased from Wacker Chemie, Munich, Germany.

Measurements

FTIR spectra were recorded on a Perkin Elmer FTIR spectrometer, Weltham, USA, using KBr as reference. The tensile tests were carried out using a universal testing machine (ZWICK-1484, Weltham, USA) at 27°C with a crosshead speed was 500 mm min^{-1} using dumbell-shaped tensile specimens according to the ASTM D 412-87. The calorimetric analysis was performed on a Netzsch differential scanning calorimeter (DSC)-200. Measurements were performed under a continuous flow of nitrogen (60 mL min^{-1}). All the samples (about 10 mg in weight) were heated from ambient to 400°C and the thermograms were recorded at a heating rate of 10°C min^{-1}. Thermogravimetric analysis (TGA) was performed on a Netzsch STA409 TGA calibrated with calcium oxalate and aluminum supplied by Netzsch, Weltham, USA. The samples (about 50 mg) were heated from ambient temperature to 600°C under a continuous flow of nitrogen (60 ml min^{-1}), at 10 C min^{-1}. The value of dielectric constant was determined with the help of an impedance analyzer (Solartron impedance/gain phase analyzer 1260, UK) using a platinum electrode at 30°C and a frequency range of 1 MHz. This experiment was repeated four times under the same conditions.

The surface morphology of the samples was examined using a scanning electron microscope (SEM; JEOL JSM Model 6360, Weltham, USA) attached with Horiba was used to record the morphology of the developed hybrid EPDM materials. Mechanical properties, namely, tensile strength, elongation at break (%), Young's modulus, and hardness of the samples, were characterized as per ASTM Standards.

Preparation of in situ eEPDM

eEPDM was synthesized via the reported procedure.[27] EPDM was dissolved in toluene in a three-necked round-bottomed flask equipped with a mechanical agitator and thermometer and maintained at 50°C in a water bath. With constant agitation, the EPDM solution was acidified by adding 88% formic acid dropwise till to obtain the pH 2–3. The epoxidation was performed by the slow addition of the calculated amount of H$_2$O$_2$ (30%) over a period of 30 min to achieve the effective epoxidation. The reaction was continued for 7 h at 50°C. After the epoxidation, the product resulted was coagulated in acetone, systematically washed with distilled water, drenched in 1% w/v Na$_2$CO$_3$ solution for 24 h, and finally rinsed with distilled water. eEPDM rubber obtained was dehydrated in a vacuum oven at 40°C to obtain a constant weight.

Synthesis of HTPDMS

HTPDMS was synthesized from octamethylcyclotetrasiloxane using the reported procedure.[28] Hundred grams of octamethylcyclotetrasiloxane and potassium hydroxide catalyst (0.22% on the weight of octamethylcyclotetrasiloxane) were taken in a five-necked round-bottomed flask purged with nitrogen. The temperature of the mixture was gradually raised to

90°C in a thermostatically controlled oil bath and maintained at this temperature for 4 h. The reaction mixture was cooled to 50°C to avoid frothing. After degassing, the unreacted octamethylcyclotetrasiloxane was removed by distillation, slowly raising the temperature to 180°C. The HTPDMS resulted was cooled to room temperature and stored in air tight containers for further use.

Synthesis of PU prepolymer

The synthesis of PU prepolymer was carried out using the reported procedure.[29] PU prepolymer of NCO/OH = 1.5 was prepared by reacting 1.5 equivalent of TDI (80/20 mixture of 2,4 and 2,6 isomers) and one equivalent of PPG 400 in a three-necked round-bottomed flask fixed with a thermometer, nitrogen inlet, and stirrer. The reaction was carried out at 70°C in nitrogen atmosphere for 3 h. The temperature was brought down to 40°C and DBTDL (0.02% w/w based on polyol) was added to the reaction mixture and stirring was continued for another 30 min. The PU prepolymer resulted was collected and preserved in a sealed container for subsequent use. The composition of synthesized PU prepolymer is presented in Table 2.

Preparation of hybrid EPDM /PU matrices

The hybrid EPDM/PU (eEPDM-*g*-APTES/HTPDMS/PU) matrix system was developed in two stages. In the first stage, 10 g of eEPDM dissolved in 200 ml toluene was taken in a 500 ml three-necked round-bottomed flask equipped with a reflux condenser, a Teflon-coated mechanical stirrer, and a nitrogen inlet. Then, 0.25 wt% of APTES was mixed with 0.75 wt % HTPDMS and dissolved in 50 ml of toluene. The resulting blend was added to eEPDM. Then, 0.02 wt% DBTDL catalysts was also added to the above mixture and continuously stirred for 2 h at 80°C after the completion of reaction. In the second stage, varying weight percentages of PU prepolymer (0.75, 1.5, 2.25, and 3.0 wt%) was reacted with hybrid EPDM (eEPDM-*g*-APTES/HTPDMS) at 80°C in the presence of DBTDL catalyst with continuous agitation for 30 min under nitrogen atmosphere. The product resulted was degassed to remove the entrapped air from the hybrid EPDM/PU matrices. The preparation of hybrid eEPDM-*g*-APTES-HTPDMS/PU matrices is presented in Figure 1.

Results and discussion

Spectroscopic analysis

Figure 2(a) illustrates the FTIR spectrum of HTPDMS: –OH stretching vibration appears in the region of 3400–3600 cm^{-1}, C–H stretching vibration at 2960 cm^{-1}, Si–O–Si symmetric stretching vibration at 1021 cm^{-1}, Si–O–Si asymmetric stretching vibration at 1098 cm^{-1}, Si–CH$_3$ bending vibration at 1260 cm^{-1}, and Si–CH$_3$ rocking vibration at 801 cm^{-1}. FTIR spectrum of hybrid EPDM (eEPDM-*g*-APTES/HTPDMS) is presented in Figure 2(b). The bands obtained are C–H stretching vibration at 2937 cm^{-1}, OH stretching vibration at 3360 cm^{-1}, and C–N stretching vibration at 1374 cm^{-1}. Disappearance of –Si–O–CH$_2$CH$_3$ peak of eEPDM-*g*-APTES at 2900 cm^{-1} and the formation of Si–O–Si asymmetric stretching vibration appeared at 1105 cm^{-1} confirm the completion of reaction between HTPDMS and eEPDM-*g*-APTES.

Figure 2(c) describes the FTIR spectrum of PU prepolymer: N–H stretching vibration at 3236 cm^{-1}, C–H stretching vibration at 2855 cm^{-1}, C=O stretching vibration of urethane at 1720 cm^{-1}, C–C stretching vibration of aromatic ring at 1560 cm^{-1}, free NCO asymmetric stretching at 2252 cm^{-1}, and C–O–C asymmetric stretching of aliphatic ether appeared at 1030 cm^{-1}. FTIR spectrum of hybrid EPDM/PU (eEPDM-*g*-APTES/HTPDMS/PU) matrices is presented in Figure 2(d). The data obtained are N–H stretching vibration at 3344 cm^{-1}, C–H stretching vibration (aliphatic) at 2909 cm^{-1}, –CH$_2$ rocking vibration at 1461 cm^{-1}, CH$_3$ symmetric bending vibration at 1374 cm^{-1} due to propylene group, –(CH$_2$)$_n$– wagging vibration at 721 cm^{-1} due to polyethylene chain, C–C stretching vibration at 2851 cm^{-1}, C–C stretching vibration of aromatic ring at 1549 cm^{-1}, and C–O–C asymmetric stretching of aliphatic ether at 1051 cm^{-1}. The disappearance of the absorption band for isocyanate groups at 2252 cm^1 and formation of C=O stretching vibration of urethane at 1718 cm^{-1}, C–N stretching vibration at 1374 cm^{-1}, and N–H peaks at 3310 cm^{-1} and 1549 cm^{-1}, respectively, ascertained the completion of the reaction. This confirms the formation of –NHCOO group in hybrid EPDM/PU matrices.

Figure 2(d) shows the FTIR spectra of hybrid EPDM/PU matrices with 2.25 wt% of PU. The major point derived from here is the intensity of isocyanate absorption peak appeared at 2252 cm^{-1} gradually decreases as the PU ratio increases from 0.75 wt% to 1.50 wt% and completely disappears when the hybrid EPDM/PU matrices are having 100/2.25 wt% (Figure 3(d)). The formation of C=O stretching vibration of urethane appeared at 1718 cm^{-1}, C–N stretching vibration at 1374 cm^{-1}, and N–H peaks appeared at 3310 cm^{-1} and 1549 cm^{-1}, respectively, indicates the completion of the reaction.

Mechanical properties

The mechanical properties obtained for EPDM, eEPDM, eEPDM-*g*-APTES/HTPDMS, and eEPDM-*g*-APTES/HTPDMS/PU hybrid are presented in Table 1. It was observed that the values of tensile strength, elongation at break
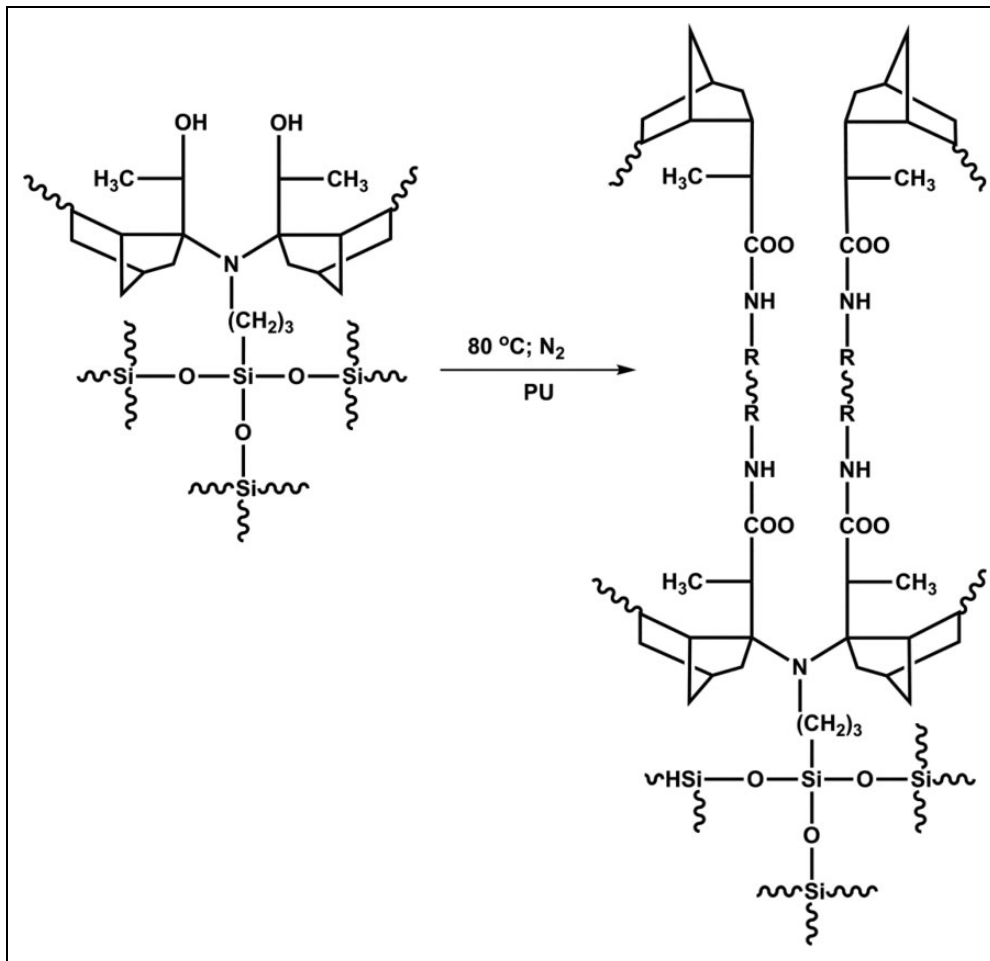
Figure 1. Preparation of hybrid eEPDM-*g*-APTES-HTPDMS/PU matrices.
eEPDM: epoxidized of ethylene–propylene–diene monomer; APTES: 3-aminopropyltriethoxysilane; HTPDMS: hydroxyl terminated polydimethylsiloxane; PU: polyurethane.
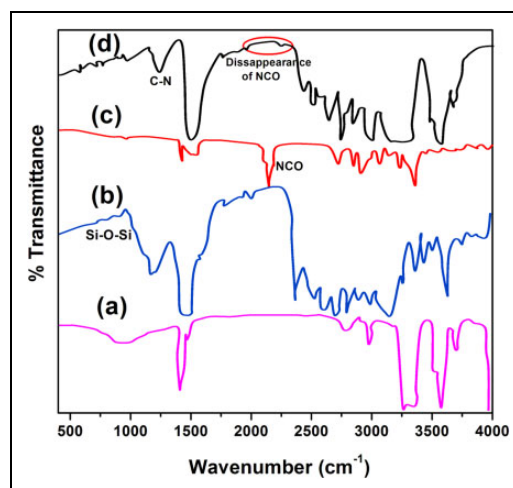

Figure 2. FTIR spectra of (a) HTPDMS, (b) hybrid EPDM, (c) PU, and (d) hybrid EPDM/PU matrices (100/2.25).
FTIR: Fourier transform infrared; HTPDMS: hydroxyl terminated polydimethylsiloxane; EPDM: ethylene–propylene–diene monomer; PU: polyurethane.

(%), and hardness of eEPDM are lowered by 7.0%, 25.9%, and 2.8%, respectively, than that of unmodified EPDM due to the introduction of epoxide groups and in turn induce the realignment of molecular structure, whereas the reverse trend in the value of Young's modulus is observed and is increased by 6.2%. Similar observation was reported for epoxidized natural rubber.
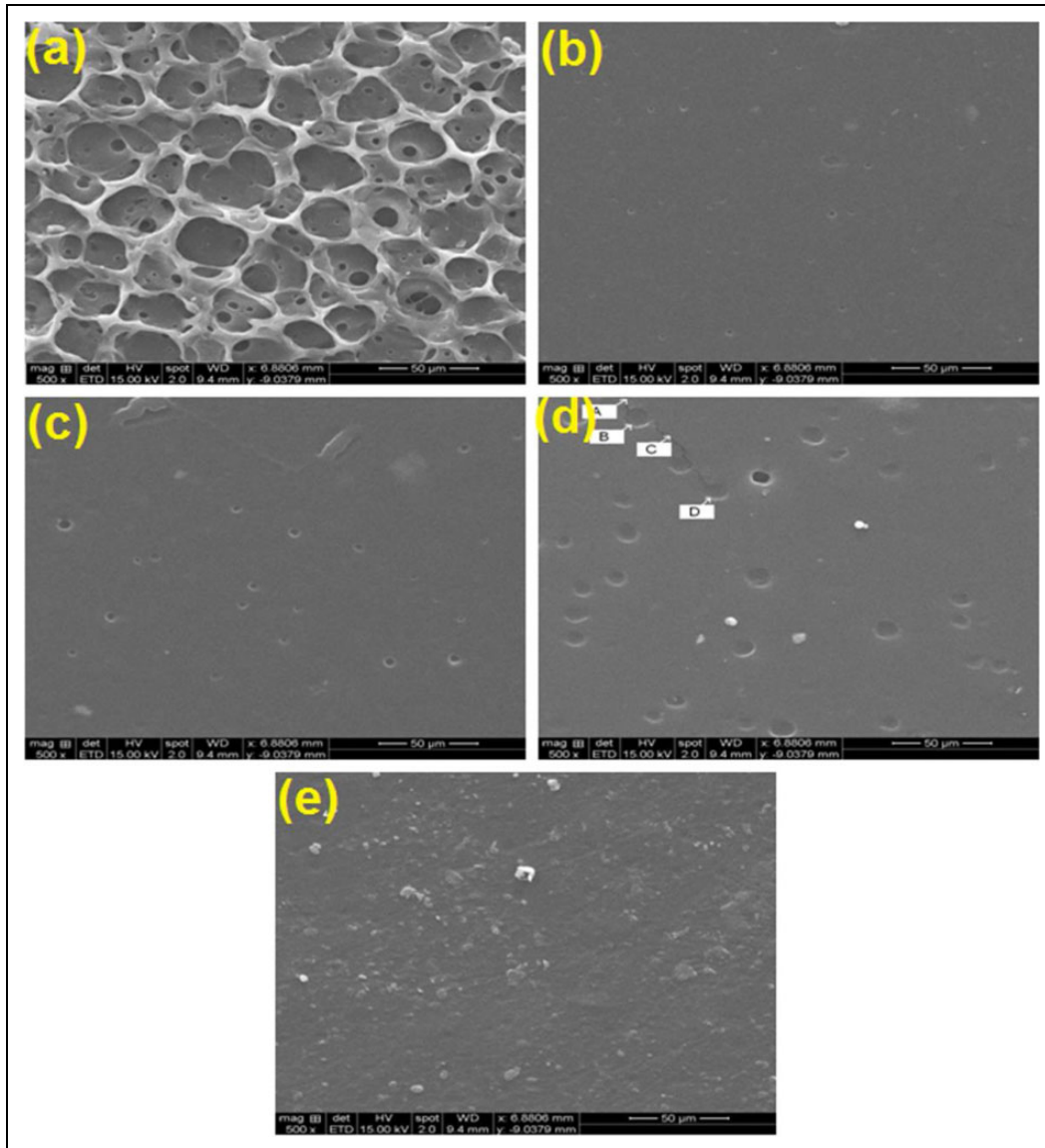
Figure 3. SEM images of (a) eEPDM-*g*-APTES/HTPDMS, (b) eEPDM-*g*-APTES/HTPDMS/PU (0.75 wt%), (c) eEPDM-*g*-APTES/HTPDMS/PU (1.5 wt%), (d) eEPDM-*g*-APTES/HTPDMS/PU (2.25 wt%), and (e) eEPDM-*g*-APTES/HTPDMS/PU (3 wt%).
SEM: scanning electron microscope; eEPDM: epoxidized of ethylene–propylene–diene monomer; APTES: 3-aminopropyltriethoxysilane; HTPDMS: hydroxyl terminated polydimethylsiloxane; PU: polyurethane.

Table 1. Mechanical properties of composites.

Components		Tensile strength (MPa)	Elongation at break (%)	Young's modulus (MPa)	Hardness (shore A)
EPDM		17.11	540	27.17	71
eEPDM		15.91	400	28.86	69
eEPDM-*g*-APTES/HTPDMS		12.70	487	20.19	59
eEPDM-*g*-APTES/HTPDMS/PU	0.75 wt%	13.50	520	23.15	64
	1.50 wt%	13.24	545	22.65	65
	2.25 wt%	12.86	562	22.20	65
	3 wt%	12.60	586	21.86	67

EPDM: ethylene–propylene–diene monomer; eEPDM: epoxidized of ethylene–propylene–diene monomer; APTES: 3-aminopropyltriethoxysilane; HTPDMS: hydroxyl terminated polydimethylsiloxane; PU: polyurethane.

The blending of eEPDM-*g*-APTES/HTPDMS with urethane prepolymer also exhibits the chain extension and flexibility induced by the urethane linkages. It was also observed that the incorporation of PU prepolymer to eEPDM-*g*-APTES/HTPDMS decreased the values of tensile strength, Young's modulus, and hardness with the enhancement in the value of elongation at break (%) according to the wt% concentration (Table 1).
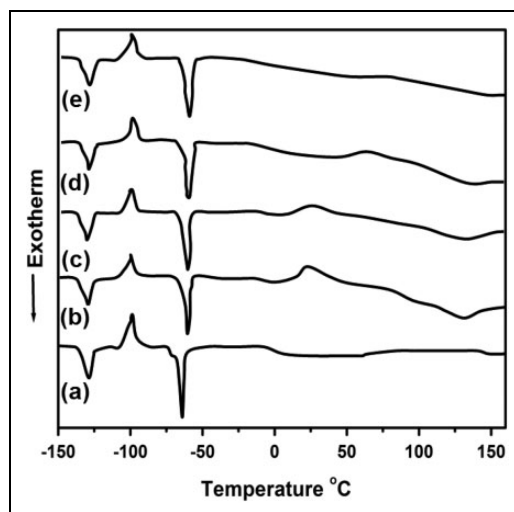
Figure 4. DSC curves of (a) hybrid EPDM, (b) hybrid EPDM/PU matrices (0.75 wt% PU), (c) (1.5 wt% PU), (d) (2.25 wt% PU), and (e) (3.0 wt% PU).
DSC: differential scanning calorimetry; EPDM: ethylene–propylene–diene monomer; PU: polyurethane.

Data resulted from mechanical studies indicate that the modification and hybridization make the EPDM become more flexible and soft than that of unmodified EPDM, which is better suitable for high-performance industrial applications.

Morphological properties

The morphology of eEPDM-*g*-APTES/HTPDMS (Figure 3(a)) shows a deformation surface with cavities in HTPDMS phase. It can also be observed that the inner surfaces of the cavity are rough with white spots that look like the bubbles escape from the surface. It was further observed that the incorporation of HTPDMS into eEPDM-*g*-APTES imparts heterogeneous morphology.

The morphology of eEPDM-*g*-APTES/HTPDMS/PU (Figure 3(b) to (e)) hybrids also exhibits heterogeneous morphology. However, unlike the morphology of eEPDM-g-APTES/HTPDMS, the morphology of hybrid PU, the HTPDMS segment is uniformly distributed over the whole hybrid matrix system, due to the fact that HTPDMS is chemically bonded between eEPDM-*g*-APTES and urethane prepolymer. The morphology of hybrid with 1.5 wt% PU possesses featureless morphology, except a crack tip area. Hybrid with 3 wt% PU matrix possesses the rough texture morphology.

Differential scanning calorimetry

Data obtained from the DSC analysis for hybrid EPDM (eEPDM-*g*-APTES/HTPDMS) are presented in Figure 4(a). Two values of glass transition temperatures (T_g) are observed in hybrid EPDM. The higher transition temperature corresponds to the EPDM phase ($T_g -65°C$), whereas the lower transition temperature corresponds to the PDMS phase ($T_g -125°C$). The value of T_g of the EPDM phase in the hybrid EPDM is significantly decreased, which indicates the partial miscibility between eEPDM-*g*-APTES and PDMS by chemical bonding. Similar observations were also reported for poly(ethyleneglycol)-polydimethylsiloxane amphiphilic block copolymers.[30]

The DSC data of hybrid EPDM with different concentrations of PU (0.75, 1.5, 2.25, and 3.0 wt%) are given in Figure 4(b) to (e). The main factors affecting the T_g are the crosslinking density and morphological structure. In hybrid EPDM/PU matrices, together with the strong polar and rigid aromatic ring, urethane and hydrogen bonds are formed between the molecules, all these form hard segment microarea. The weak EPDM chains, PDMS phase, C–N bonds, and C–O bonds form the soft segment phase. Although there is a certain degree of compatibility between soft and hard segment, the hard segment and soft segment phases are incompatible due to the nature of thermodynamics, resulting in microphase separation. The soft segment phase and hard segment phase show respective T_g. The DSC thermograms of hybrid EPDM containing PU clearly show the T_g of PDMS soft segment at $-125°C$, indicating that the PDMS microphase separated from both the EPDM soft segment and the hard segment phase. The broad transitions at $-55°C$ might be due to the glass transition of the EPDM. The value of T_g of PU hard segment varies from $111°C$ to $120°C$, depending on the PU content, indicating that the PU microphase is separated from both the PDMS and the EPDM soft segments.

Thermal stability

Thermal stability of modified and hybridized EPDM was determined using TGA, and the results, namely, decomposition temperature (T_d) and char yield (%), obtained are presented in Table 2. The blending of eEPDM-*g*-APTES/HTPDMS with

Table 2. Thermal and dielectric properties of composites.

Components		T_g (°C)	T_d (°C)	Char yield (%) at 600°C	Dielectric constant (ε)
EPDM		−58	490	9.3	3.14
eEPDM		−55	482	8.6	3.46
eEPDM-*g*-APTES/HTPDMS		−65, −125	512	24.3	3.10
eEPDM-*g*-APTES/HTPDMS/PU	0.75 wt%	−125	495	19.6	3.40
	1.50 wt%	−55	489	20.4	3.45
	2.25 wt%	−111	486	21.8	3.54
	3 wt%	−120	480	22.6	3.63

EPDM: ethylene–propylene–diene monomer; eEPDM: epoxidized of ethylene–propylene–diene monomer; APTES: 3-aminopropyltriethoxysilane; HTPDMS: hydroxyl terminated polydimethylsiloxane; PU: polyurethane.

varying wt% of urethane polymer marginally lowers the values of T_d and char yield (%) due to the presence polar urethane linkages, which are more vulnerable for decomposition than that of siloxane linkages. Observation similar to this was reported by Ramar et al.[31,32]

Dielectric behavior

Synthetic polymers are widely used as electrical insulators for different industrial and engineering applications. Further, the incorporation of inorganic crosslinker into thermoplastics produces three-dimensional network structures with adequate thermal endurance behavior coupled with good electrical and mechanical properties suitable for cable insulates.

In the present study, EPDM was suitably modified and hybridized with silane, HTPDMS, and urethane prepolymer and the value of dielectric constant was determined using solartron impedance analyzer, and the results obtained are presented in Table 2. It was observed that the value of dielectric constant of EPDM was marginally decreased when it was epoxidized (eEPDM) due to the formation of polar epoxide groups, whereas the decrease in the value of dielectric constant was noticed when eEPDM was grafted with APTES due to the hydrophobic behavior imparted by the silane moiety and incorporation of HTPDMS into eEPDM-*g*-APTES/HTPDMS also lowers the value of dielectric constant to an insignificant extent due to the enhancement of hydrophobic behavior and the development of heterogeneous domains with the formation of voids in the hybrid eEPDM-*g*-APTES/HTPDMS system. Further, the incorporation varying wt% of urethane prepolymer into eEPDM-*g*-APTES/HTPDMS increases the value of dielectric constant according to the concentration. This may be explained due to the increase in the number of polar urethane sites with the formation of hydrogen bonding in the system. The modification and hybridization of EPDM through epoxidation, grafting, and blending marginally alter the value of dielectric constant according to the nature and concentration of the components involved.

Data resulted from thermal and dielectric studies indicate that the modification and hybridization of EPDM improved both thermal and insulating behavior to an appreciable extent than that of unmodified EPDM and these results suggest that the hybridized EPDM can be considered as a better material for high-performance cable insulation applications.[33,34]

Conclusion

Hybrid siliconized–epoxidized EPDM/PU matrices were developed using eEPDM with 2.5 wt% of APTES as crosslinker and varying weight percentages (0.75, 1.5, 2.25, and 3.0 wt%) of urethane prepolymer as chain extender and toughener along with fixed weight percent (7.5 wt%) of HTPDMS as impact modifier at appropriate experimental conditions. The molecular structure, morphology, thermal, dielectric, and mechanical properties of the hybrid matrices were characterized using different analytical methods. The epoxidation of EPDM, hybridization of APTES grafted eEPDM with HTPDMS, and urethane prepolymer were carried out in a sequential manner and the formation of hybrid matrices through chemical linkages with components involved is ascertained by FTIR. Data resulted from morphological analysis indicate that the components in the hybrid matrices are uniformly distributed in the continuous matrix system with phase-separated heterogeneous morphology due to the presence of hydrocarbon and siloxane segments.

The T_g of APTES grafted eEPDM enhanced from −55°C to −48°C and that of urethane hybridized eEPDM increased from 111°C to 120°C due to the formation of crosslinked network structure and intermolecular hydrogen bonding, It was also observed that the incorporation of APTES, urethane prepolymer, and HTPDMS improved the elongation at break (%) and marginally lowered the values of tensile strength, Young's modulus, and hardness according to the percentage concentration. Data resulted from different studies indicated that the siliconized hybrid eEPDM/PU matrices developed in the present work can be considered as an effective replacement for conventional EPDM and can be used as high-performance cable insulation materials under different environments.

Declaration of conflicting interests

The author(s) declared no potential conflicts of interest with respect to the research, authorship or publication of this article.

ORCID iD

Manokaran Vadivel https://orcid.org/0000-0002-2173-6960

References

1. Ram R, Rahaman M and Khastgir D. Mechanical, electrical, and dielectric properties of polyvinylidene fluoride/short carbon fiber composites with low-electrical percolation threshold. *J Appl Polym Sci* 2013; 131(3): 39866, (1–10).
2. Ram R, Rahaman M and Khastgir D. Electrical properties of polyvinylidene fluoride (PVDF)/multi-walled carbon nanotube (MWCNT) semi-transparent composites: modelling of DC conductivity. *Compos A* 2015; 69: 30–39.
3. Ram R, Rahaman M, Aldalbahi A, et al. Determination of percolation threshold and electrical conductivity of polyvinylidene fluoride (PVDF)/short carbon fiber (SCF), composites: effect of SCF aspect ratio. *Polym Int* 2017; 66(4): 573–582.
4. Rahaman M. Physical properties of polyvinylidene fluoride/multi-walled carbon nanotube nanocomposites with special reference to electromagnetic interference shielding effectiveness. *Adv Polym Technol* 2018; 37: 3287–3296.
5. Ram R, Khastgir D and Rahaman M. Electromagnetic interference shielding effectiveness and skin depth of polyvinylidene fluoride—particulate nano carbon fillers composites: prediction of electrical conductivity and percolation threshold. *Polym Int* 2019; 68(6): 1194–1203.
6. Sethi D, Ram R and Khastgir D. Analysis of electrical and dynamic mechanical response of conductive elastomeric composites subjected to cyclic deformations and temperature. *Polym Compos* 2017; 39(11): 3912–3923.
7. Sethi D, Ram R and Khastgir D. Electrical conductivity and dynamic mechanical properties of silicon rubber based conducting composites: effect of cyclic deformations, pressure, and temperature. *Polym Int* 2017; 66(9): 1295–1305.
8. Jiang J, Xu J-S, Zhang Z-S, et al. Rate-dependent compressive behavior of EPDM insulation: experimental and constitutive analysis. *Mech Mater* 2016; 96: 30–38.
9. Rallini M, Puri I, Torre L, et al. Effect of liquid resol on the mechanical and thermal properties of EPDM/kynol elastomeric heat shielding materials. *Polym Eng Sci* 2017; 57: 513–520.
10. Vadivel M, Shobana S, Narayan SA, et al. Optimization of process conditions and characterization of ethylene-propylene-diene rubber with bismaleimide. *Bulg Chem Commun* 2017; 49: 26–30.
11. Riba Ruiz J-R, Canals T and Cantero R. Supervision of Ethylene Propylene Diene M-Class (EPDM) rubber vulcanization and recovery processes using Attenuated Total Reflection Fourier Transform Infrared (ATR FT-IR) spectroscopy and multivariate analysis. *Appl Spectrosc* 2017; 71: 141–151.
12. Ning N, Qin Ma, Zhang Y, et al. Enhanced thermo-oxidative aging resistance of EPDM at high temperature by using synergistic antioxidants. *Polym Degrad Stab* 2014; 102: 1–8.
13. Livanova NM, Popov AA, Shershnev VA, et al. Modification of ethylene-propylene-diene elastomers to improve the ozone resistance of their covulcanizates with butadiene-nitrile rubbers. *Polym Sci Ser A* 2011; 53:133–142.
14. Ravanbakhsh M, Khorasani SN and Khalili S. Blending of NR/BR/ENR/EPDM-g-GMA by reactive processing for tire sidewall applications: effects of grafting and ENR on curing characteristics, mechanical properties, and dynamic ozone resistance. *J Elastomers Plast* 2016; 48: 394–403.
15. Choi SS and Kim JC. Thermal aging behaviors of weather resistant rubber composites of EPDM, IIR, and BIIR. *J Elastomers Plast* 2012; 47: 148–155.
16. Lin CW, Chien CH, Tan J, et al. Dynamic mechanical characteristics of five elastomeric gasket materials aged in a simulated and an accelerated PEM fuel cell environment. *Int J Hydrogen Energy* 2011; 36: 6756–6767.
17. Kommling A, Jaunich M and Wolff D. Effects of heterogeneous aging in compressed HNBR and EPDM O-ring seals. *Polym Degrad Stab* 2016; 126: 39–46.
18. Pourmand P, Linde E, Hedenqvist MS, et al. Profiling of thermally aged EPDM seals using portable NMR, indenter measurements and IR spectroscopy facilitating separation of different deterioration mechanisms. *Polym Test* 2016; 53: 77–84.
19. Natali M, Rallini M, Puglia D, et al. EPDM based heat shielding materials for solid rocket motors: a comparative study of different fibrous reinforcements. *Polym Degrad Stab* 2013; 98: 2131–2139.
20. Natali M, Rallini M, Kenny J, et al. Effect of Wollastonite on the ablation resistance of EPDM based elastomeric heat shielding materials for solid rocket motors. *Polym Degrad Stab* 2013; 130: 47–57.

21. Natali M, Puri I, Rallini M, et al. Ablation modeling of state of the art EPDM based elastomeric heat shielding materials for solid rocket motors. *Comp Mater Sci* 2016; 111: 460–480.

22. Mead J.L, Tao Z and Liu H.S. Insulation materials for wire and cable applications. *Rubber Chem Technol* 2002; 75(4): 701–712.

23. Sameh ZAD, Illias HA, Ang BC, et al. Electrical properties of polyethylene/polypropylene compounds for high-voltage insulation. *Energies* 2018; 11: 1448,(1–13).

24. Ekelund M, Fantoni PF and Gedde UW. Thermal ageing assessment of EPDM-chlorosulfonated polyethylene insulated cables using line resonance analysis (LIRA). *Polym Test* 2011; 30: 86–93.

25. Shen L, Xia L, Han T, et al. Improvement of hardness and compression set properties of EPDM seals with alternating multilayered structure for PEM fuel cells. *Int J Hydrogen Energy* 2016; 41: 23164–23172.

26. Sarac T, Quievy N, Gusarov A, et al. The study of temperature and radiation induced degradation of cable polymers: a comparison between the mechanical properties of industrial and neat EPDM. *Proc Struct Int* 2016; 2: 2405–2414.

27. Ao YH, Sun SL, Tan ZY, et al. Compatibilization of PP/EPDM blends by grafting acrylic acid to polypropylene and epoxidizing the diene in EPDM. *J Appl Polym Sci* 2006; 102: 3949–3954.

28. Serier A, Pascault JP and My LT. Reactions in aminosilane–epoxy prepolymer systems I. Kinetics of epoxy–amine reactions. *J Polym Sci Part A Polym Chem* 1991; 29: 209–218.

29. Ng SC and Gan LH. Reaction of natural rubber latex with performic acid. *Eur Polym J* 1981; 17: 1073–1077.

30. Rutnakornpituk M, Ngamdee P and Phinyocheep P. Synthesis, characterization and properties of chitosan modified with poly (ethylene glycol)-polydimethylsiloxane amphibhilic block copoloymers. *Polym* 2005; 46: 9742–9752.

31. Ramar P and Alagar M. Studies on grafting of tris(2-methoxyethoxy)vinylsilane onto ethylene-propylene-diene terpolymer. *Polym Adv Technol* 2004; 15: 377–381.

32. Alagar M, Abdul Masjid SM and Nagendiran S. Preparation and characterization of vinyltriethoxysilane grafted ethylene propylene diene terpolymer/linear low density polyethylene (EPDM-g-VTES/LLDPE) blends. *Polym Adv Technol* 2005; 16: 582–591.

33. Canaud C, Antonio Sens M, Yuan Visconte LL, et al. EPDM formulations for electric wires and cables. *Kaut Gummi Kunstst* 2001; 54: 56–60.

34. Ku CC. and Liepins R. Tangent of dielectric loss angle of polymers. In: Verlog CH (ed) *Electrical properties of polymers: chemical principles*. New York, NY: Hanser Publishers, 1987, p. 181.